PERIODICO di MINERALOGIA
established in 1930

DIPARTIMENTO
DI SCIENZE DELLA TERRA

SAPIENZA
UNIVERSITÀ DI ROMA

An International Journal of
Mineralogy, Crystallography, Geochemistry,
Ore Deposits, Petrology, Volcanology
and applied topics on Environment, Archaeometry and Cultural Heritage

Chemical and Mineralogical Characterization of Malaysian Low-Grade Manganese Ore

Suhaina Ismail, Syed Fuad Saiyid Hashim, Hashim Hussin, Norazharuddin Shah Abdullah*

School of Materials and Mineral Resources Engineering, Universiti Sains Malaysia, Engineering Campus, 14300 Nibong Tebal, Penang, Malaysia

ARTICLE INFO

Submitted: September 2016
Accepted: October 2016
Available on line: November 2016

* Corresponding author: azhar.abdullah@usm.my

DOI: 10.2451/2016PM612

How to cite this article:
Ismail S. et al. (2016) Period. Mineral. 85, 277-288

ABSTRACT

This paper aims to chemically and mineralogically characterize the Malaysian low-grade manganese ore (LGMO). The optical microscope, and scanning electron microscope (SEM) equipped with an energy-dispersive X-ray analyzer (EDX) were used for ore morphology assessment, mineral liberation analysis, particle texture studies, grain size distribution and mineral association assessment. X-ray fluorescence (XRF) and X-ray diffraction (XRD) were used to determine the LGMO's composition and to identify mineral phases, respectively. SEM images with EDX analysis revealed various optical characteristics of the ore, while XRF results showed that the major elements present in this LGMO are Si, (mean value of 16.95 wt%), followed by Mn, Fe, and Al (at mean values of 13.17 wt%, 4.63 wt%, and 4.70 wt%, respectively). Phase analysis by XRD meanwhile revealed the presence of α-quartz, pyrolusite, and aluminum-substituted goethite. The natural grain-size distribution and texture (observed using optical and backscattered image analysis) revealed that manganese liberation was observed at particle sizes below 150 μm. This indicates that particle size has a significant effect on the recovery of the manganese oxide. The data and information obtained from this characterization study will aid in the identification and the design of a suitable treatment method for this local LGMO, and with that, the possibility of exploiting this deposit as a local source of manganese.

Keywords: Low-grade manganese ore; ore characterization; mineral liberation; Scanning Electron Microscopy; X-Ray Diffraction and Fluorescence; Rietveld refinement.

INTRODUCTION

World production of manganese (Mn) ore in 2010 rose by 26% on a gross weight basis, and by 31% on a contained-weight basis, compared to that in 2009 (Corathers, 2012). Nonetheless, the current worldwide Mn production is still unable to cope with the demand from the growing metallurgical industry. It is reported that metallurgical applications of manganese consume 77% to 90% of the total Mn ore production (Corathers, 2012). Mn is mainly used as a deoxidizer and desulfurizer in steel making, and as an important component in alloy-making. Other than that, additional quantities of manganese were used for non-metallurgical purposes such as a component in dry cell batteries, an additive in plant fertilizers and animal feed, as well as a colorant (for bricks) in the production of masonry (Corathers, 2012).

As reported in Mineral Commodity Summaries (2012), no satisfactory substitute exists for replacing Mn with other metals in its major applications. As the number of products from Mn applications continues to rise, the demand for Mn continues to increase. However, the metal's supply remains limited. Due to that, the price of Mn escalated over the years, and some deposits, which were previously considered low-grade, can now be economically mined (Abou-El-Sherbini, 2002; El Tawil et al., 1989; Hariprasad et al., 2007).

Enrichment of low-grade ores, however, is not trivial. One fundamental importance in the development and

operation of mining and mineral processing systems, especially for low-grade or complex ores, is the classification and characterization of minerals (Ismail et al., 2015; Olubambi et al., 2008a). Characterization is pivotal as it will heavily influence the process flow design for the recovery/enrichment of constituent metals.

It is known that different minerals from various locations have unique mineralogical composition with varying characteristics and complexities. At this point, it is expected that the understanding of mineralogy, chemical composition, size, morphology and association with other minerals, through in-depth characterization, will provide an indication/basis on the mineral's behaviour during beneficiation and recovery processes (Olubambi et al., 2008a).

In this paper, the above-mentioned local LGMO was characterized. The LGMO characterization includes by particle size analysis, X-ray fluorescence (XRF), X-ray diffraction (XRD), and scanning electron microscopy (SEM) with energy dispersive X-ray analyzer (EDX); each to determine particle size distribution, elemental composition, mineral phases which are present within the ore, and the ore morphological conditions, respectively. These details will undoubtedly assist in the understanding of the ore itself, to be potentially exploited as a new resource of heavy minerals in Malaysia.

MATERIALS AND METHODS

Geological setting

Sungai Temau is situated at the northern part of the state of Pahang, within the district of Kuala Lipis. Somewhat in central region of peninsular Malaysia, it is approximately 40 km southwest of Gunung Tahan, the highest point on the Malaysian peninsular. The site is also approximately 35 km slightly northeast of Selinsing, and about 45 km slightly northwest of Penjom, both Selinsing and Penjom are famous local gold-mining areas. With reference to Figure 1, Selinsing is labelled 4, while Penjom is labelled as 6. Visually, the mapped location of Sungai Temau in Figure 1 is roughly in the middle of points 3 and 4, (i.e., Ketok Baru and Selinsing, respectively) as per the solid, black circle.

The geology of northern Pahang (inclusive of Sungai Temau) was thoroughly discussed, amongst others by Yeap (1993), Tan and Lim (1990) and as early as Hutchinson (1973). It is evident that the literature suggested that the northern Pahang area is divided into Devonian metasediments, acid and intermediate intrusive

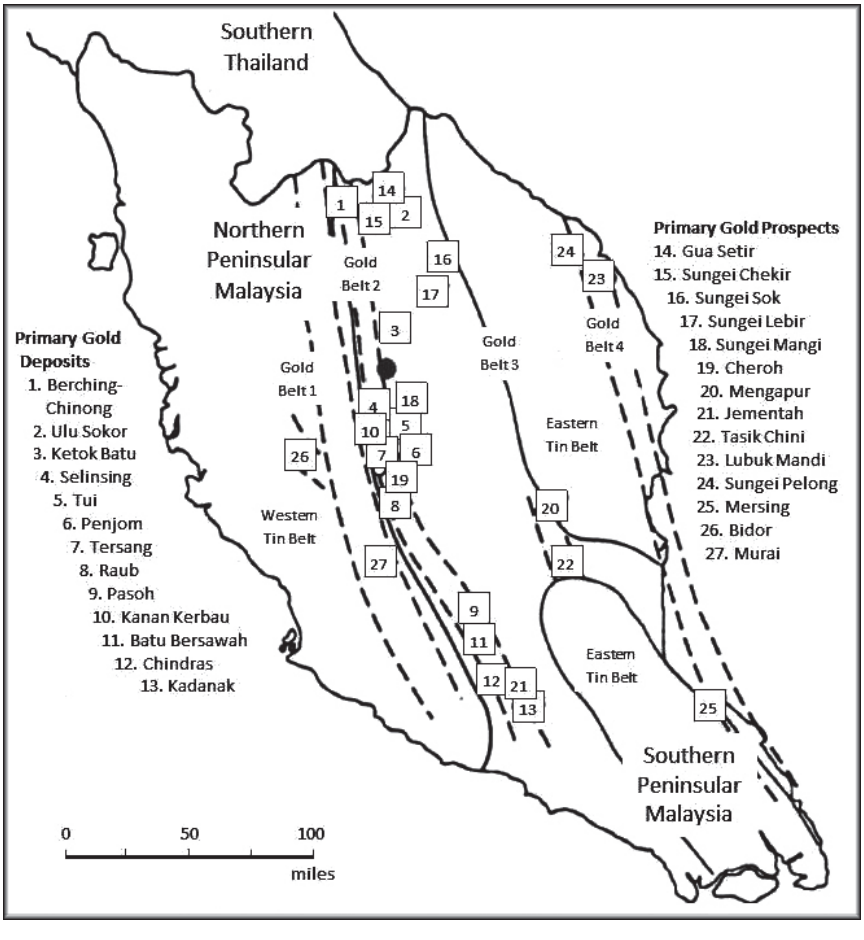

Figure 1. The Peninsular Malaysia with the various Tin and Gold Belts. The approximate location of Sungai Temau (labelled as the solid, black circle), which is in the middle of Selinsing (point 4) and Ketok Batu (point 3). (modified from Ariffin, 2012).

structures and various sections of argillaceous, calcareous and volcanic Permian facies. Ariffin (2012) showed that argillaceous and calcareous Permian facies are the larger and more obvious structures, as seen in Selinsing, Tui and Penjom (i.e., points 4-6 in Figure 1), up to Pulai, to just before the acidic intrusive sections of Ketok Batu (point 3). The same was also suggested by Tan and Lim (1990), with clear indication that other than the Gua Musang formation in Merapoh (nearby Ketok Batu) are largely argilites southwards. Thus, it is expected that the ores obtained from Sungai Temau would also be either calcareous or argillaceous, with the latter being more prominently suggested geologically.

Sample preparation

Sample preparation was done as per Figure 2, before commencing with the characterization efforts. Representative samples of the bulk LGMO were collected from the ore site (located nearby Sungai Temau, Pahang). Prior to comminution, the ore samples were screened, visually assessed and were sampled. Due to the wide size range of the obtained field samples, stratified sampling was done, with each fraction being weighed and then sampled individually.

The coarse particles from Sungai Temau, at -120 mm, were crushed in a jaw crusher (i.e., secondary crushing, with an average size reduction ratio of 6:1) followed by crushing in a cone crusher (i.e., tertiary crushing, with an average size reduction ratio of 5:1). The oversized particles (+4.00 mm) in this case were returned for further tertiary crushing. The crushed ore with sizes below 4.00 mm, meanwhile, were ground for further size reduction (i.e., using ceramic ball mill). Size analyses of crushed and ground products were done by laboratory test screening. One representative portion (obtained after going through the riffle box) was analyzed for particle

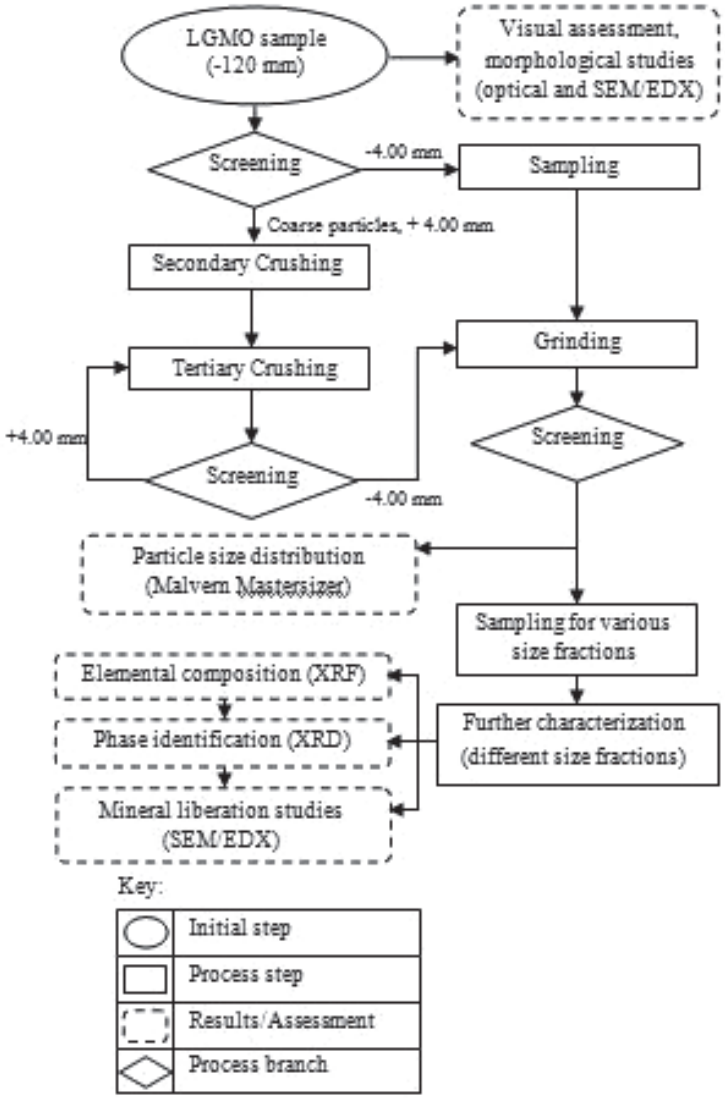

Figure 2. A flowchart depicting the stages involved in the characterization of Malaysian low-grade manganese ore (LGMO) in this work.

size analysis. Another sampled portion was screened to multiple fractions (-500+350) µm, (-350+250) µm, (-250+150) µm, (-150+75) µm, and -75 µm, and each was subsequently analyzed for elemental composition, identification of mineral phases, morphological conditions and liberation studies, respectively.

Ore visual assessment and ore morphological studies

LGMO samples were visually scrutinized and preliminary morphological studies were done via optical image analysis. Samples were mounted with sufficient epoxy resin and hardener in a matrix, were subsequently cut, and followed by mechanical polishing. Initial polishing was achieved with a rotary grinder (Metaserv), using 180, 320, 600, 1000 silicon carbide grits, followed by diamond lap polishing with oil-based lubricant. The specimens then were washed with ethanol, prior to visualization of optical properties and surface morphology.

An Olympus BX41 reflected light microscope was used for optical images of the bulk LGMO. This microscope has a stabilized 100W halogen illumination for reflected light microscopy, providing high intensity and sharp images. However, to accurately identify and quantify mineral abundance and liberation, the sample is required to be analysed with FESEM/EDX (Zeiss Supra 35VP-24-58). The samples were observed and imaged at a 10mm working distance and 15 kV accelerating voltage. In this work, back-scattered electron (BSE) images were utilized to ascertain the physical properties of minerals, while EDX provided information on their chemistry. For SEM/EDX analysis, all the samples were coated with gold/palladium alloy (Au/Pd) via sputtering to improve surface conductivity.

Particle size distribution (PSD)

Ground ore samples were subjected to particle size distribution analysis using Malvern Mastersizer E, which applies a laser diffraction method. The analyzed powder was put in de-ionized water and mixed with 20% of calgon. Then, in a recirculating cell, the entire sample passes through the laser beam and diffraction is obtained from all the particles. Cumulative size distribution and volume distribution graphs were generated directly. The d_{90}, d_{50}, d_{10} values represent the 10^{th}, 50^{th} and 90^{th} percentile of cumulative passing and, volume moment diameter (VMD) was calculated by Malvern Mastersizer's software (v2.15). The span value (ψ) meanwhile, for a sample distribution, is defined as equation (1), as follows:

$$\Psi = \frac{d_{90}-d_{10}}{2d_{50}} \qquad (1)$$

Elemental composition (using X-ray fluorescence)

Determination of the elemental composition of the ore was performed by X-ray Fluorescence Spectroscopy using Rigaku RIX 3000 XRF spectrometer. The XRF spectrometer was equipped with Rh X-ray tube, 4 kW generator and an interface to PC with RIX being the software on a Windows platform. Samples at -75 µm were further ground using agate mortar for homogenization, and to minimize any scattering effect. The homogenized samples were hydraulically pressed into pellets under the pressure of 60 kN for one minute, in triplicates. The pellets were then exposed to the primary X-ray beam for elemental analysis, with semi-quantitative analyses to follow.

Mineral phase identification (using X-ray diffraction)

The identification of phases present in the powdered sample was done using Bruker D8 Advanced X-ray diffractometer with a Cu-anode and Kα radiation. Particulate samples of -75 µm were used for the qualitative and quantitative analysis of the minerals within the ore. The X-ray diffractometer was operated at a generator voltage of 40 kV and a current of 30 mA with the 2θ values varying from 20º to 70º. The counting time, meanwhile, was fixed to 1s for each 0.034º of the 2θ step. The identification of all minerals was done with PANalytical X'Pert HighScore Plus software (v2.2e) and PANalytical ICSD database. Generally, most ore samples have high background readings due to the high degree of overlapping peaks. Thus, background corrections were made, as suggested McCusker et al. (1999), to remove the background noise from the XRD patterns. Full profile fitting of the diffractogram was made by progressively refining parameters such as intensities of individual mineral phases, unit cell dimensions, peak widths, preferred orientations, and global parameters like zero setting of the diffractometer, utilizing the Rietveld refinement algorithm (McCusker et al., 1999). All these parameters were used for the simulation of peak shapes which in turn, will be used to generate a calculated diffraction pattern. The calculated diffraction pattern is then compared with the observed data, and the differences between the observed and calculated were minimized. At the end of each stage of refinement, the weight percent of each mineral phase is obtained.

Mineral liberation studies

As shown in Figure 2, mineral liberation was assessed using SEM/EDX analysis on polished section specimens at different size fractions. In this study, 9 size fractions were chosen, which are: (-4.00+3.35) mm, (-3.35+2.8) mm, (-2.80+1.18) mm, (-1180+500) µm, (-500+350) µm, (-350+250) µm, (-250+150) µm, (-150+75) µm, and -75 µm, respectively. As reported by Olubambi et al., (2008a) the degree of liberation was estimated using equation (2).

$$\% \text{ Mineral liberation} = \frac{FM}{FM+LM} \times 100 \quad (2)$$

Where:

FM= Total area of mineral particles (of interest) which are liberated

LM= Total area of mineral particles (of interest) in locked form

The areas of liberated and locked particles (representatively sampled) wezre assessed and the total areas were estimated and calculated, effectively yielding the degree of liberation.

RESULTS AND DISCUSSIONS

Visual assessment of Sungai Temau's LGMO

Prior to size reduction, the received LGMO samples were observed visually under ordinary light. The subjective assessments were done on samples as displayed in Figure 3. It is observed that the raw (field) samples were -120 mm in size, and irregular in shape. This implies that a reliable crushing and grinding stage is needed for size reduction before processing takes place. The colour seems to vary from light grey to darker grey, to brownish, and some areas being blackish, greyish and cream, with granular features being noted. The varying colour possibly indicates that the bulk LGMO samples are a mixture of various minerals. It is well known that manganese may occur in a few major forms, such as pyrolusite (MnO_2) as the most common, with braunite ($Mn^{2+}Mn^{3+}{}_6$)(SiO_{12}) and especially rhodochrosite ($MnCO_3$) being less common. As it is believed that no independent manganese mineral is found in the main stage of magmatic crystallization (Supriya, 1981), thus, heavy association of these manganese minerals to amongst others, iron/phosphorus/aluminum-bearing and/or silicate minerals are not unusual. This association was explained in detail as early as Reed (1960), Buckenham (1961), and as recent as Kholodov and Nedumov (2009) and Siddiquie et al. (2015) for various manganese deposits worldwide.

Figure 3. Visual assessment of Malaysian low-grade manganese ore (LGMO) samples obtained for this work.

The granular feature of the dark greyish section, where the streak appears dark grey to dark bluish, may suggest the presence of pyrolusite, which is a major manganese ore. Brownish sections, with a black streak, may suggest some iron-rich mineral, based on the fact that it is common for manganese to associate with iron ore bodies, which are enriched during its transformation (Pontus, 1960; Buckenham, 1961; Supriya, 1981). The grey and cream regions on the LGMO samples may be silicate minerals of some type, based on the fact that the location of Sungai Temau strongly suggests that the LGMO deposit may originate within argillized rock masses. It is conceded, however, that this visual assessment may only serve as a guide. Identification of each mineral type, present within the ore in question, should be confirmed by quantitative and qualitative means (e.g., XRD and XRF), before any conclusions can be drawn.

Ore morphological studies

Qualitative optical characteristics (e.g., colour, shape and mineral association) were distinguished by reflected light microscope. Microscopic studies on different areas in the same sample revealed different mineral associations, clearly depicted in Figure 4a and Figure 4b.

In Figure 4a, the ore sample is observed to be made of a sequence of dark grey to black layers, entwined with white to pinkish sections, forming an alternately layered formation. Via EDX, these dark grey to black layers are determined (at this stage) as Mn-rich phase, with a presence of iron, while the white to pinkish sections are identified as Si-dominant phases. Figure 4b shows Si-rich sections (within the investigated LGMO sample) as the dominant gangue mineral, with Mn dissemination/filling. This particular texture in Figure 4b is a common occurrence of manganese ore (i.e., secondary formation) originated within argillized rocks (where the Si-rich phases are usually quartz). This is in agreement with what was mentioned in the Geological Setting and Visual Assessment sections, where it was suggested that the occurrence of this LGMO deposit may lie within argillized wall-rocks. Other than that, the results from this optical study indicate that mineral liberation may be very challenging in this case, due to ore association complexity (i.e., bedding/alternating-layers and disseminated Mn in Si-rich regions). Further qualitative assessment for mineral identification, in this case, can be supplemented by quantitative assessment via SEM back-scattered image (BSI). The supplementary mineralogical information was obtained from BSIs by SEM/EDX analysis as in Figure 5.

A low-noise, high-resolution image is a prerequisite for mineral identification and quantification. Different morphologies were observed at LGMO sample mounted

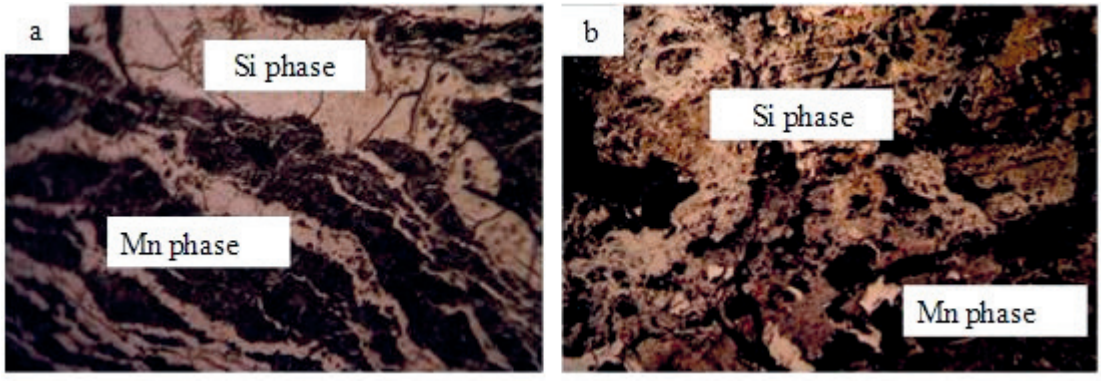

Figure 4. Images from the optical microscope, depicting the complexity of mineralogy and the multiple textures of Malaysian low-grade manganese ore (LGMO). (a) Zoning structure of Mn and Si phases, (b) Disseminated Mn phase in Si-rich phase. Elemental determination was done by EDX.

in resin showing colour discrimination, as displayed in Figures 5 a-c. The main components identified in those figures (via EDX) are essentially manganese rich mineral (i.e., possibly pyrolusite, with shades of light grey to cream) as a major phase, associated with Si-rich regions (dark grey) and aluminium-iron rich mineral (light grey). Other elements, which may be present in trace amounts, were not detected by this SEM/EDX analysis. Again, the results support the initial visual assessment, as previously stated in the previous paragraphs.

Figure 5a shows a very fine Mn-rich grain intergrowth in the Si-rich gangue region. Figure 5b meanwhile, displays fibrous Mn-rich zones containing aluminium-iron phases and Figure 5c displays a likely zoning occurrence of Mn-rich regions with aluminium-iron phases. The different grey shade levels in LGMO samples are reflecting compositional variations of Mn, Fe, Al and Si content. With reference to the compositional variations in LGMO particle, the Mn, Fe, Al and Si contents were assayed by EDX linescan in Figure 6.

Figure 6 clearly depicts the compositional variation across an ore sample. It is clear here, that the whitish

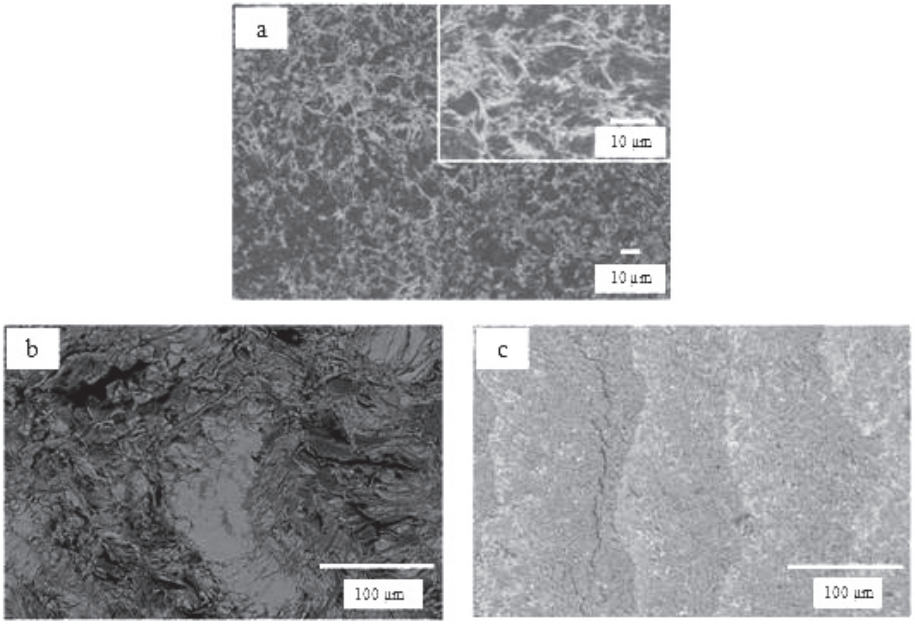

Figure 5. Backscattered imaging (BSI) of (a) Very fine manganese and aluminium-iron phase's intergrowth in quartz gangue, (b) fibrous manganese-rich phase containing aluminium-iron phases, (c) zoning structure of different grey levels of manganese and aluminium-iron phases from the optical microscope, depicting the complexity of mineralogy and the multiple textures of Malaysian low-grade manganese ore (LGMO). (a) Zoning structure of Mn and Si phases, (b) Disseminated Mn phase in Si-rich phase. Elemental determination was done by EDX.

region is manganese-rich, enclosed within a light grey layer, which is identified as an iron-rich constituent. The surrounding regions, depicted as mixed shades of darker grey with an appearance of undulating texture are Si and Al-rich. This texture would have resulted from the weathering process, by which pyrolusite and goethite formed during a late phase of the alteration in the iron ore and argillized wall-rocks. This further supports the results reported in previous sections. During weathering, replacement of one mineral by another or by a mineral may result from oxidation, dissolution and precipitation or solid state diffusion. From the above observation, the LGMO sample can be characterized as a sedimentary deposit in nature with Mn-Fe-Al-Si association. Variation

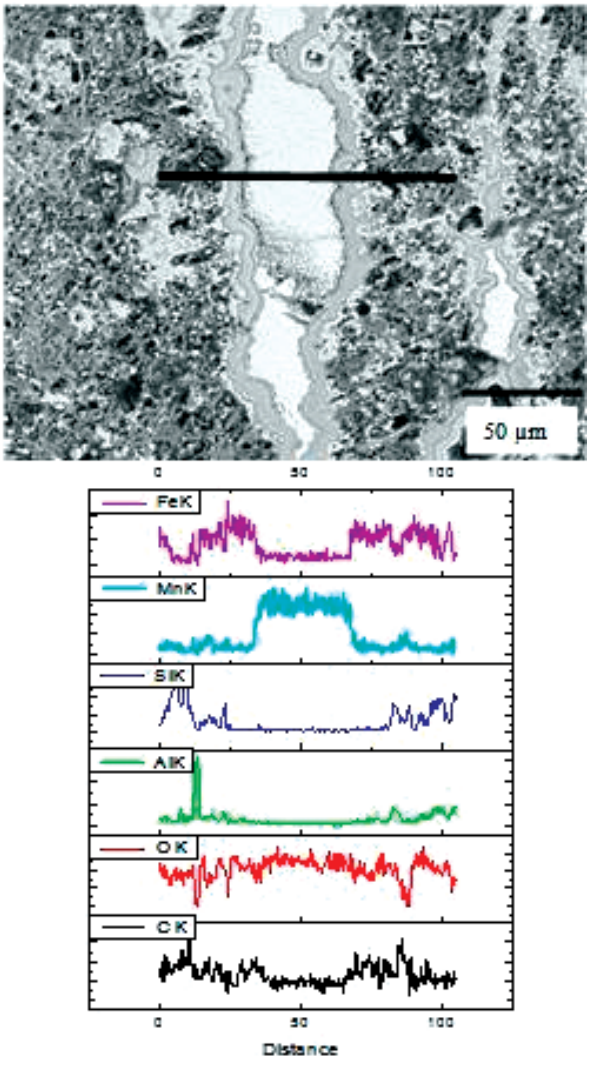

Figure 6. (Top) Backscattered imaging (BSI) of the Malaysian LGMO and (bottom) EDX linescan analysis showing compositional variation within the LGMO sample. X-axis caption 'Distance' refers to µm, similar to the scale in the BSI.

in chemical composition of these phases suggests that bulk compositions of the host rock have played an important role in the formation of these phases during metamorphism (Shah and Moon, 2004).

Particle size distribution (PSD)

The size range of the product after grinding is an important assessment, especially in relation to determining the extent of mineral liberation via comminution. Figure 7 shows a cumulative passing (%) and volume (%) particle size distribution of the LGMO in question. The cumulative passing sizes were measured by Malvern Mastersizer Version 2.15 software, revealing that the values of d_{90}, d_{50} and d_{10} are 143.98 µm, 59.09 µm and 11.3 µm, respectively. From these values, the width of particle size distribution, or expressed as span value was calculated as 143.88 using equation (2). This relatively high span value indicates a wide size distribution after comminution. A good agreement is also shown by volume (%) particle size distribution, in which a multimodal distribution was observed. Therefore, the volume moment diameter of 67.8 µm calculated by the same particle size distribution estimation software was taken as the mean diameter for this type distribution.

Elemental composition analysis (XRF)

The typical classification of manganese ore (which can later be translated into possible uses in applications), is based on its manganese content and the presence of other constituents within the ore. Thus, for classification purposes (amongst others), determination of elements present in Sungai Temau's LGMO is essential. Table 1 shows the average elemental composition in the LGMO obtained from XRF analysis, taken from 10 random but representative LGMO samples.

XRF analysis confirmed that the elements present in the ore are Si (at 16.95%), followed by Mn, Fe and Al at 13.17%, 4.63% and 4.70%, respectively. Other elements such as K, Ti, Mg, Ca and Na were also detected, but present in trace levels (less than 1%). As mentioned by Pontus (1960), a remarkably low content of Mg in LGMO (less than 15%) can be explained by mineral formation conditions and mechanisms. The elemental composition confirms that the sample obtained from Sungai Temau is indeed a low-grade manganese ore, which further supports the preliminary visual assessment and ore morphological studies presented in the previous sections. The results also pointed out that the Sungai Temau LGMO can be metallurgically classified as a ferruginous type manganese ore. The ferruginous ore is classified based on the Mn content (i.e., first-grade ore > 48% Mn, second grade having 48-45% Mn, third grade having 44-35% Mn, ferruginous ore having 34-10% Mn, while manganiferous ores having less than 10% Mn). Clear presence of Al, Si,

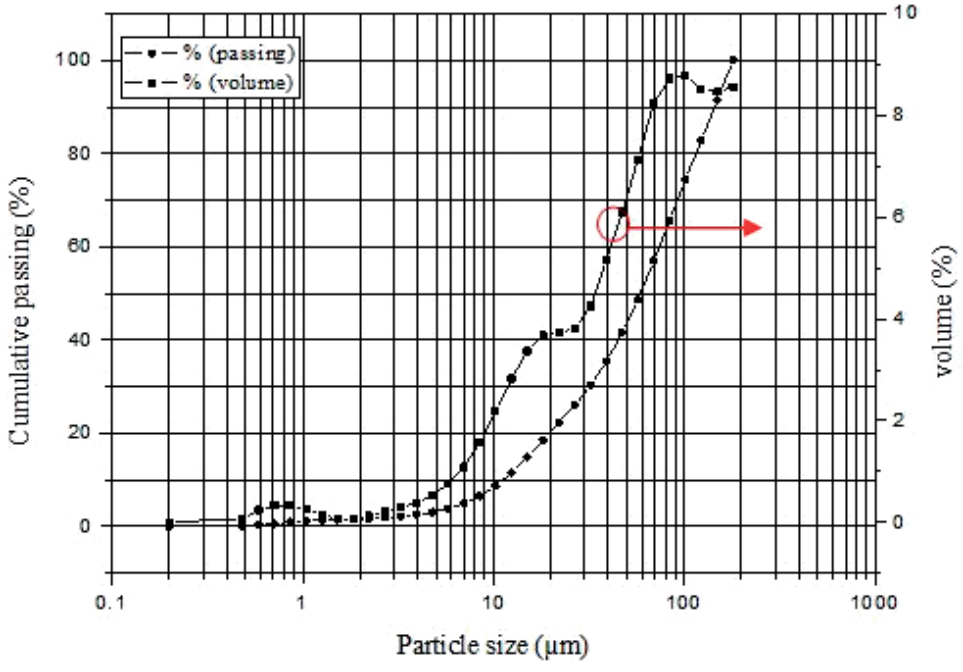

Figure 7. Particle size distribution (PSD) of ground LGMO with cumulative and volume distribution curves.

Table 1. The average elemental composition (from ten random representative samples) of Malaysian low-grade manganese ore (LGMO) from Sungai Temau, Pahang, in the central region of peninsular Malaysia.

Particle size	% Weight								
	Mn	Si	Fe	Al	K	Ti	Mg	Ca	Na
(≤75µm)	13.17	16.95	4.63	4.70	0.92	0.31	0.21	0.073	0.04

Ti, Mg, Ca, and Na may denote argillization, which is consistent with the geological setting of the area where the ore samples were obtained. What is of certainty, the presence of quite a number of elements within the ore adds to the ore complexity and possible intricateness in the possible recovery of manganese from the ore.

Identification of mineral phases

Generally, XRD is a reliable tool for common mineral identification. However, in low-grade ore with complex minerals (i.e., a number of phases may occur), the challenge of mineral identification should be noted. The mineral phase identification was done by controlling the search-match parameter within the PANalytical X'Pert HighScore Plus software. It is apparent that most of the mineral phases were in line with ICSD reference database. As shown in Figure 8, the XRD pattern obtained revealed that Sungai Temau's LGMO consists of pyrolusite (ICSD-98-003-5167), α-quartz (ICSD-98-001-2466) and Al-substituted goethite (ICSD-98-009-8759). Rietveld refinement (separation of overlapping peaks, structure determination, phase conformation and quantitative phase analysis) was performed after phase identification. In utilizing this refinement method, the mineralogical knowledge of low-grade manganese ore is imperative for phase confirmation after possible identification. The important corrections have been applied during the refinement and these are adopted from McCusker et al. (1999). Thus, the mineralogical knowledge of low-grade manganese ore is much needed during the phase identification and Rietveld refinement stages, as explained in the following paragraphs.

In this study, the determination of pyrolusite as one of the minerals within the said LGMO is not as straightforward as the determination of α-quartz. Although pyrolusite is known to be the most stable manganese oxide, in various circumstances, pseudomorphic replacements of other manganese oxides (e.g., manganite) may occur. It is noted

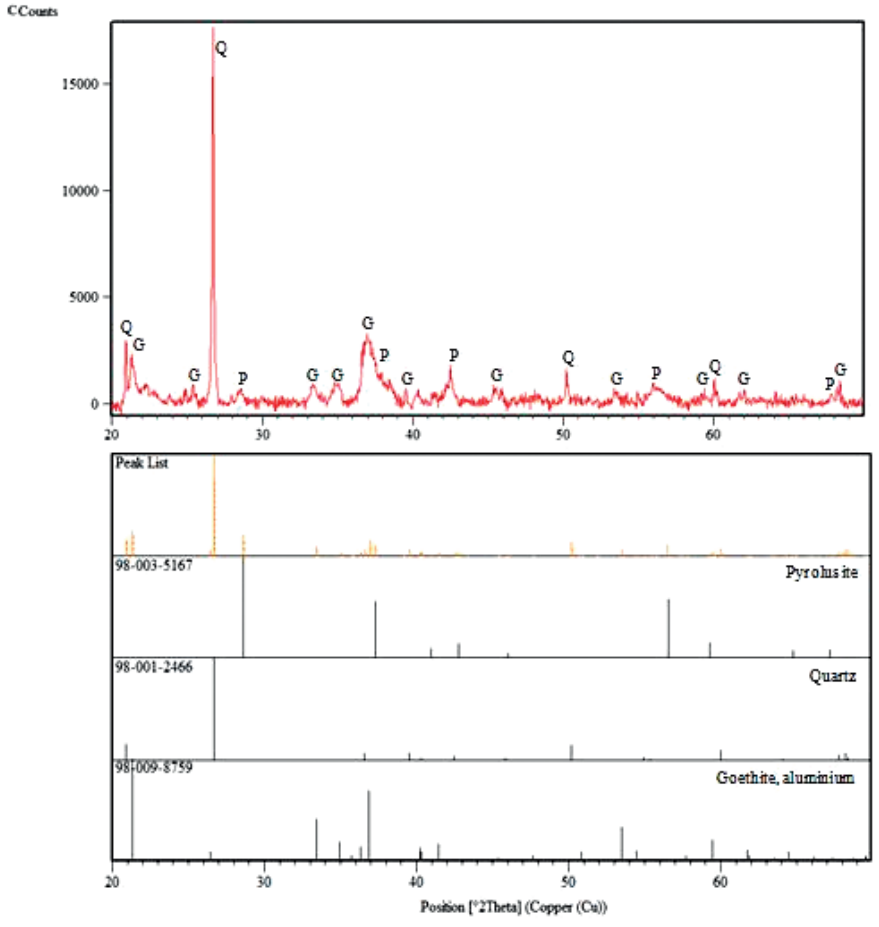

Figure 8. A sample XRD pattern of the Malaysian low-grade manganese ore (LGMO) in question. Abbreviations: Q, Quartz; P, Pyrolusite; G, Aluminium-substituted goethite.

that both pyrolusite and manganite have a nearly same structure and an orientation of similar unit cell dimensions (Rask and Buseck, 1986). Thus, in this case, depending solely on simple/initial Rietveld refinement may not be sufficient for phase identification. Unit cell refinement needs to be done in order to distinguish between pyrolusite and manganite phases. In this study, this was successfully done, providing proof of pyrolusite presence, instead of manganite.

Al-substituted goethite determination was also not straightforward. For to detect the substituted goethite phases, a two step-refinement, i.e., of unit cell and site occupancies were done, due to possible solid solution occurrence (Kirwan et al., 2009 and Schulze, 1984). According to Schulze (1984) Al substitution in goethite varies among different geological environments, the Al substitution ranges between 0 to 33 mol %. As the Al^{3+} ion is slightly smaller that the Fe^{3+} ion (i.e., 0.53 Å vs 0.65 Å in radii), Al substitution for Fe in the goethite structure, reduces the average size of the unit cell. The influence of Al substitution in goethite is well documented in previous studies (Schulze, 1984), and can be clearly indicated by shifts of the goethite X-ray diffraction lines to smaller d-values. After structure refinement, Al-substituted goethite was identified.

The overall degree of refinement in the Rietveld analysis is judged by the goodness of fit (*s*), which is a ratio of weighted profile R-factor (R_{wp}) to the expected R-factor (R_{exp}). Determination of acceptable values of *s*, and R_{wp} and R_{exp}, for that matter, was thoroughly discussed by Toby (2006) and is not repeated here for brevity. Nonetheless, it is known that R_{wp} values should not be smaller than that of R_{exp}, and it is desirable to have an *s* value close to 1 (i.e., R_{wp} and R_{exp} values should be close) to demonstrate excellent refinement through the Rietveld method. In this work, acceptable values were obtained, with R_{wp}=2.87%, R_{exp}=2.01%, giving *s* as 1.43. From this quantitative phase analysis, it may be safely concluded that the LGMO from Sungai Temau consists of 59.3% α-quartz, 14.8% pyrolusite and 25.9% Al-substituted goethite.

Mineral distribution and liberation

Liberation analysis is a very useful tool in mineralogy, especially when applied to mineral processing. Liberation analysis provides information that cannot be obtained by other analytical techniques such as XRF and XRD. The cost of liberation analysis becomes negligible when it is considered that the data obtained often results in modifications being made to plant operations, for a positive economic impact in the region of millions of dollars (in the long run). Because of the comparatively high cost of size reduction, and the difficulties associated with separating minerals when over or under liberation occurs, it is essential that the optimum amount of size reduction can be achieved (Lastra, 2007; Olubambi et al., 2008b). With the help of SEM/EDX, a good estimation on the optimum size reduction to liberation correlation can be obtained. The SEM/EDX micrographs of the selected size fractions are shown in Figure 9, each revealing the qualitative mineral liberation characteristics of the LGMO investigated in this work.

Figure 9 a-d show that unliberated manganese particles are mostly within very coarse to medium particles in size. At these size fractions, major constituents of the ore are observed to be closely associated with very little liberation. For example, Figure 9b depicts an unliberated Mn-rich grain (identified as pyrolusite with goethite association), blanketed by quartz externally. Further size reduction results in reduced quartz blanket thickness, clearly shown in Figures 9 c-f. It is noted that at these size fractions, rectilinear particle boundaries and occlusion sections are clearly observed. Increased liberation can be achieved by further reduction of the rectilinear boundaries; arguably, in ore particles showing occlusion in phases, further size reduction may result in incomplete mineral separation, although high enough liberation still may occur. In the LGMO investigated, signs of good manganese phase liberation are observed at sizes less than 150 µm, as shown in Figures 9 h-i.

The measurements of liberation degree were carried out as described previously, using equation (2) and the results of the analyses are shown in Figure 10. Based on these results, the liberation for manganese phase in

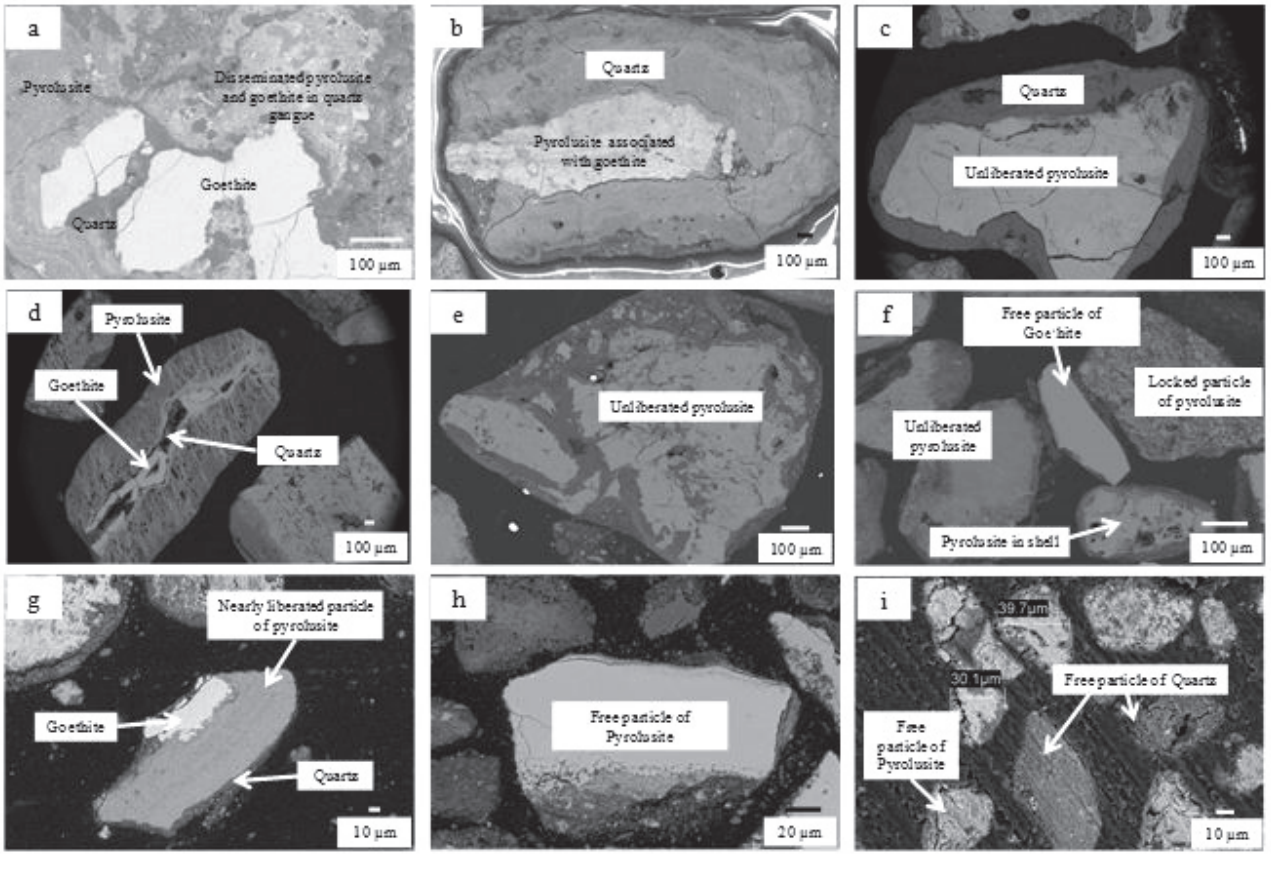

Figure 9. Nine samples of random backscattered imaging (BSI) of Malaysian low-grade manganese ore (LGMO), done to distinguish the degree of mineral liberation at different LGMO size fractions. (a) Refers to (-4.00+3.35)mm, (b) (-3.35+2.8)mm, (c) (-2.80+1.18) mm, (d) (-1180+500)µm, (e) (-500+350)µm, (f) (-350+250)µm, (g) (-250+150)µm, (h) (-150+75)µm, and (i) -75µm.

Sungai Temau's LGMO initiates after grinding to sizes of -250+150 µm. At 150 µm, approximately 60% manganese phase liberation was observed, while further grinding up to 75 µm liberates approximately 80% of the available manganese phase (oxide). At -75 µm, LGMO particles exhibit excellent manganese phase liberation (~92%).

These results also suggest that this local LGMO occur as locked particles within coarser fractions (i.e., 300 µm and 250 µm), and mineral liberation starts after size reduction to -150 µm, as seen in Figure 8(h). Unsurprisingly, the degree of liberation seems to increase with size reduction, although excessive grinding (finer than 75 µm) may not be necessary to obtain liberated ore particles. In general fine particle separation is difficult since entrainment of gangue particles in concentrate easily occurs (Ito et al., 2008; Olubambi et al., 2008b). Finally, it is heavily portrayed here that any effort to recover Mn from this LGMO may need a decent amount of grinding. It is imperative that grinding should be done to the size of at least (-150+75) µm, in order to obtain good Mn liberation (about 80%). At this size fraction and liberation percentage, extractive efforts through chemical leaching look realistic. Nonetheless, it is known that leaching of pyrolusite (even fully liberated) may not be straightforward. Other considerations such as the usage of reduction agents, good agitation, and higher temperatures need to be taken into consideration to ensure acceptable and economical recovery of Mn from this Malaysian LGMO.

CONCLUSIONS

The Malaysian LGMO is characterized. The complexity of Malaysian LGMO is due to Mn-Al-Fe-Si associations (determined through EDX), with layered zoning, intergrowth, disseminated and fibrous structures (determined through optical microscope/SEM). These structures are clearly observed in the ore, which displayed granular features, and mostly irregular in shape. The grinding stage revealed good size reduction, samples with a d_{90} value of 143.98 µm, d_{50} of 59.09 µm and d_{10} of 11.3 µm were collected (via Malvern Mastersizer). The wide size range, nonetheless, may suggest a more controlled grinding scheme needs to be put in place. Elements present within the LGMO were revealed by XRF analysis. The major elements present in the ore are Si, Mn, Fe and Al, each averaging at 16.95 wt%, 13.17wt%, 4.63 wt%, and 4.70 wt%, respectively. Other elements such as K, Ti, Mg, Ca and Na were found to be present in trace amounts (less than 1 wt%). This result indicates that the LGMO can be metallurgically classified as ferruginous manganese ore, based on the percentage of Mn present. XRD analysis meanwhile revealed that revealed that the main ore mineral is pyrolusite, together with α-quartz and aluminum-substituted goethite. This supports the XRF and EDX findings. Rietveld analysis indicates that the ore contains α-quartz (59.3%), pyrolusite (14.8%) and aluminum-substituted goethite (25.9%), with values of R_{wp} (2.87%) and R_{exp} (2.01%). The complexity of the ore itself (i.e., structure, feature and phases present), suggests the bulk composition of the host rock have played a major role in the formation of this ore. Although complex, the Mn in LGMO may be liberated with ample grinding. At the size range of (-150+75) µm, approximately 80% pyrolusite particles are seen liberated. Further grinding (sizes less than 75 µm) yielded 90% (approximate) liberation of pyrolusite. The high removal of locked particles at this particular size range suggests that Mn may be recovered from the LGMO via hydrometallurgical route. It is however known that chemical leaching of Mn from pyrolusite is not straightforward. Thus, proper experimental efforts should be carried out to determine the viability of the process.

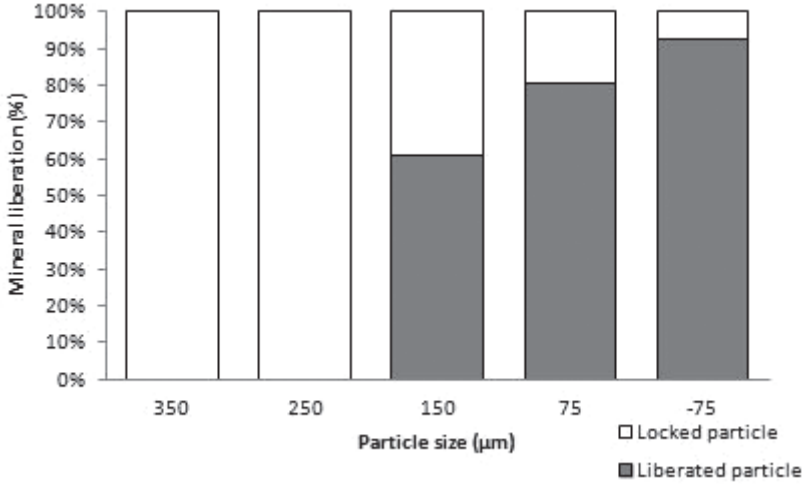

Figure 10. Percentage of liberation obtained from image analysis of particles as per Figure 9 (e-i), i.e., particle size fractions of (-500+350) µm, (-350+250) µm, (-250+150) µm, (-150+75) µm, and -75 µm, respectively. Percentage of liberation was calculated as per equation (2).

ACKNOWLEDGEMENTS

The authors gratefully acknowledge the support provided by Universiti Sains Malaysia (USM) through USM's Short Term research grant (304/PBAHAN/60313029). The technical support from Mr. Kemuridan Mat Desa, Ms. Haslina Zulkifli and Mdm. Fong Lee Lee is also much appreciated.

REFERENCES

Abou-El-Sherbini K.S. (2002) Simultaneous extraction of manganese from low grade manganese dioxide ore and beneficiation of sulphur slag. Separation and Purification Technology 27, 67-75.

Ariffin K.S. (2012) Mesothermal Lode Gold Deposit Central Belt Peninsular Malaysia. In Dr. Imran Ahmad Dar (Ed.) Earth Sciences, ISBN: 978-953-307-861-8, InTech, 313-342.

Buckenham M.H. (1961) Beneficiation of manganese ores with particular reference to the treatment of a low grade ore from Viti Levu, Fiji, New Zealand Journal of Geology and Geophysics 4, 136-147.

Corathers L.A. (2012) U.S Geological Minerals Yearbook-2010 (Manganese), U.S. Department of Interior and Geological Survey.

El Tawil S.Z., El Barawy K.A., Saba A.S. (1989) High-grade manganese dioxide from low-grade ores. Journal of Minerals, Metals and Materials Society 41, 38-39.

Hariprasad D., Dash B., Ghosh M.K., Anand S. (2007) Leaching of manganese ores using sawdust as a reductant. Minerals Engineering 20, 1293-1295.

Hutchinson (1973) Metamorphism. In D.J. Gobbett and C.S. Hutchison (Eds.) Geology of the Malay Peninsula. Wiley-Intersc., N.Y., 253-303.

Ismail S., Hussin H., Hashim S.F.S., Abdullah N.S. (2015) Leached Residue Characterization of Manganese-Bamboo Saw Dust Blend: An X-Ray Diffraction Study. Advanced Materials Research 1087, 370-373.

Ito M., Tsunekawa M., Yamaguchi E., Sekimura K., Kashiwaya K., Hori K., Hiroyoshi N. (2008) Estimation of degree of liberation in a coarse crushed product of cobalt-rich ferromanganese crust/nodules and its gravity separation. International Journal of Mineral Processing 87, 100-105.

Kholodov V.N. and Nedumov R.I. (2009) Association of manganese ore and phosphorite-bearing facies in sedimentary sequences: Communication 1. Parastereses and parageneses of phosphorus and manganese in Mesozoic-Cenozoic and Upper Paleozoic rocks. Lithology and Mineral Resources 44, 1-18.

Kirwan L.J., Deeney F.A., Croke G.M., Hodnett K. (2009) Characterisation of various Jamaican bauxite ores by quantitative Rietveld X-ray powder diffraction and ^{57}Fe Mössbauer spectroscopy. International Journal of Mineral Processing 91, 14-18.

Lastra, R. (2007) Seven practical applications cases of liberation analysis. International Journal Mineral Processing 84, 337-347.

McCusker L.B., Von Dreele R.B., Cox D.E., Louër D., Scardi P. (1999) Rietveld refinement guidelines. Journal of Applied Crystallography 32, 36-50.

Olubambi P.A., Ndlovu S., Potgieter J.H., Borode J.O. (2008a) Mineralogical characterization of Ishiagu (Nigeria) complex sulphide ore. International Journal of Mineral Processing 87, 83-89.

Olubambi P.A., Ndlovu S., Potgieter J.H. Borode J.O. (2008b) Role of mineralogy in optimizing conditions for bioleaching low grade complex sulphides ores. Transaction of Nonferrous Metal Society of China 18, 1234-1246.

Pontus L. (1960) Todorokite and Pyrolusite from Vermlands Taberg, Sweden. The American Mineralogist 45, 235-238.

Rask J.H. and Buseck P.R. (1986) Topotactic relations among pyrolusite, manganite, and Mn: A high resolution transmission electron microscopy investigation. American Mineralogist 71, 805-814.

Reed J.J. (1960) Manganese ore in New Zealand. New Zealand Journal of Geology and Geophysics 3, 344-354.

Schulze D.G. (1984) The influence of Aluminium on Iron Oxide. VIII. Unit cell dimensions of Al-substituted Goethites and estimation of Al from them. Clay and Clay Minerals 32, 36-44.

Shah M.T. and Moon C.J. (2004) Mineralogy, geochemistry and genesis of the ferromanganese ores from Hazara area, NW Himalayas, Northern Pakistan. Journal of Asian Earths Science 23, 1-15.

Siddiquie F.N., Alam J., Shaif M. (2015) Occurrence of Manganese Ore Deposits and Their Mineralogy in Vizianagaram-Visakhapatnam Manganese Ores Belt (Andhra Pradesh) India. International Journal of Geosciences 6, 549-566.

Supriya R. (1981) Manganese Deposit. Academic Press Inc., London.

Tan T.H. and Lim K.L. (1990) Environment of placer gold deposits in northern Pahang. Geological Society of Malaysia Bulletin 26, 1-11.

Toby B.H. (2006) R factors in Rietveld analysis: How good is good enough? Powder Diffraction 21, 67-70.

Yeap E.B. (1993) Tin and gold mineralization in Peninsular Malaysia and their relationships to the tectonic development. Journal of Southeast Asian Earth Sciences 8, 329-348.